Title: Un-steady state modeling for free cyanide removal and biofilm growth in a RBC batch process

Authors: Belén Sotomayor Burneo, A. Sánchez Juárez, Diego Alejandro Nieto Monteros

PII: S0304-3894(19)30574-6
DOI: https://doi.org/10.1016/j.jhazmat.2019.05.040
Reference: HAZMAT 20647

To appear in: *Journal of Hazardous Materials*

Received date: 21 January 2019
Revised date: 15 May 2019
Accepted date: 16 May 2019

Please cite this article as: Sotomayor Burneo B, Sánchez Juárez A, Nieto Monteros DA, Un-steady state modeling for free cyanide removal and biofilm growth in a RBC batch process, *Journal of Hazardous Materials* (2019), https://doi.org/10.1016/j.jhazmat.2019.05.040

Title: Un-steady state modeling for free cyanide removal and biofilm growth in a RBC batch process

Authors: Belén Sotomayor Burneo[a], A. Sánchez Juárez[b], Diego Alejandro Nieto Monteros[a]

Affiliation: [a]Bioprocesses Engineering Laboratory, Environmental Engineering Section, Chemical and Exact Sciences Department, Universidad Técnica Particular de Loja, San Cayetano alto s/n, P.C.: 1101608, Loja, Ecuador. mbsotomayor1@utpl.edu.ec, diego.nieto@ufpr.br, dalejandronieto@yahoo.es

[b]Physical Chemistry and Mathematics Section, Chemical and Exact Sciences Department, Universidad Técnica Particular de Loja, San Cayetano alto s/n, P.C.: 1101608, Loja, Ecuador. aasanchez11@utpl.edu.ec

Corresponding author[1]: Diego Alejandro Nieto Monteros, Bioprocesses Engineering Laboratory, Environmental Engineering Section, Chemical and Exact Sciences Department, Universidad Técnica Particular de Loja, San Cayetano alto s/n, P.C.: 1101608, Loja, Ecuador. (+593) 73701444, dalejandronieto@yahoo.es, diego.nieto@ufpr.br

Graphical abstract

[1] Present address: Diego Alejandro Nieto Monteros, Federal University of Paraná (UFPR) – Centro Politécnico, 81531-990 Curitiba, Paraná, Brazil, P.C.: 19011, (+55) 41988918785, dalejandronieto@yahoo.es / diego.nieto@ufpr.br

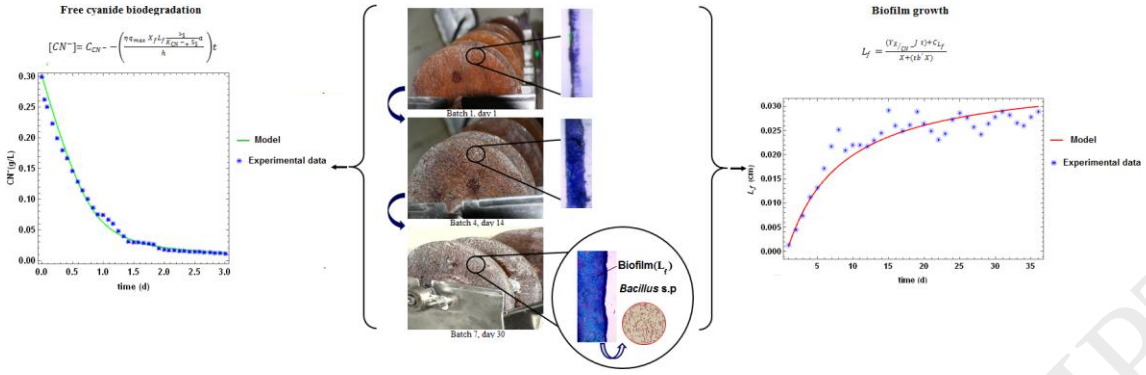

Highlights

- Biofilm used free cyanide as sole carbon and nitrogen sources.
- Free cyanide biological removal was 96.36% without additional carbon source.
- Free cyanide biodegradation model adjusted favorably to its experimental data.
- Biofilm growth model adjusted well with its experimental data.

Abstract

In this study we modeled and simulated biofilm growth and free cyanide biological removal from gold mine wastewater using a bench-scale rotating biological contactor (RBC). Eight batch cultures were run in three independent compartments (1.7L, each) of the RBC. The system worked under the following conditions: $[CN_i^-]$=0.3g/L, pH=10.5±0.5, T=20±5°C, ω=5rpm, and 40.5% of disc submersion. During each culture, biofilm thickness, biomass, and free cyanide concentration in the liquid were quantified. Subsequently, μ_{max}, K_{CN^-}, Y'_{X/CN^-}, q_{max}, b', $\mathrm{D_f}$, k, and J_{CN^-} were determined using experimental data to later model and simulate the biofilm thickness and free cyanide biological removal with Wolfram Mathematica software. After the experiments, free cyanide biological removal was 96.33% after three days, and maximum biofilm thickness was 0.0292cm in the 16th day. Moreover, biofilm growth and free

cyanide consumption models adjusted to the experimental data with r^2=0.90 and r^2=0.99. Also, there was an equivalent error of 7.89 and 7.38 and a standard deviation of 10.89% and 10.17%, between the models and their experimental data, respectively. Finally, the proposed models will allow to improve reactor operation and its design.

Keywords: Biofilm; Biological removal; Free cyanide; Mathematical model; Rotating biological contactor

Nomenclature

Symbol	Description	Unit
$\boldsymbol{\varphi}$	Association factor for the dissolvent	--
$\boldsymbol{\rho}$	Biofilm density	g/cm^3
$\boldsymbol{L_f}$	Biofilm thickness	cm
$\boldsymbol{b_{det}}$	Biofilm detachment due to shear stress	h^{-1}
$\mathbf{b'}$	Biofilm-loss coefficient	h^{-1}
$\mathbf{X_D}$	Biomass concentration on the discs	g/L
$\boldsymbol{D_w}$	Free cyanide diffusion coefficient in water	cm^2/d
$\boldsymbol{D_f}$	Free cyanide diffusion coefficient within the biofilm	cm^2/d
Z	Distance between the liquid medium and the disk	cm
μ_d	Liquid dynamic viscosity	g/cm-s
$\boldsymbol{J}$	Free cyanide flux within the biofilm	g/ cm^2-d
$[\boldsymbol{CN_i^-}]$	Initial concentration of free cyanide	g/L
$\boldsymbol{v_A}$	Kinematic viscosity	cm^2/d
$\boldsymbol{L}$	Length traveled by the biofilm in the liquid	cm
$\boldsymbol{k}$	Mass transfer coefficient	cm/d
$\boldsymbol{\mu_{max}}$	Maximum specific growth rate	h^{-1}
$\boldsymbol{q_{max}}$	Maximum specific rate of free cyanide consumption	$gCN^-/g_{biomass}$-d

$\boldsymbol{\mu}$	Microbial growth rate	h^{-1}
$\boldsymbol{M_B}$	Molecular weight of the solvent	Kg/mol
$\mathbf{Y'_{x/CN^-}}$	Observed biomass yield from free cyanide	$g_{biomass}/gCN^-$
$\boldsymbol{R_d}$	Disk radius	cm
$\boldsymbol{V}$	RBC working volume	cm^3
$\boldsymbol{Re_d}$	Reynolds number, disk	--
$\boldsymbol{\omega}$	Disk rotational speed	rpm
$\mathbf{K_{CN-}}$	Saturation constant for free cyanide	g/L
Sc	Schmidt number	--
$\boldsymbol{\sigma}$	Shear stress	g/ cm-s^2
$\boldsymbol{\mu_{dec}}$	Specific growth rate due to decay	h^{-1}
$\boldsymbol{a}$	Biomass specific area	cm^2/cm^3
$\boldsymbol{T}$	Temperature	K
dz	Differential section of the biofilm thickness	cm
$\boldsymbol{t}$	Time	d
$\boldsymbol{h}$	Water fraction from RBC total volume	--

1. Introduction

The mining-metallurgical industry uses cyanide leaching techniques for gold and silver extraction[1-3]. As a result, large volumes of effluents are generated annually, which contain high concentrations of heavy metals and hazardous compounds such as cyanide. Cyanide can be present in wastewaters in different forms like: free cyanide (CN^-), weak acid dissociable, strong cyanide complexes, among others[3, 4]. Free cyanide is highly toxic to living organisms because it inhibits cellular respiration and is considered a significant pollutant of water bodies and soils[2-10].

In order to prevent negative environmental impact from free cyanide, physico-chemical and biological treatments have been developed[3, 4, 11]. Physico-chemical treatments present some

disadvantages including generation of harmful by-products, high operational costs, and difficulty of maintenance[3, 11, 12]. On the other hand, biological treatments are efficient, economical, and environmentally friendly[1, 2, 4, 12-16].

Free cyanide biological removal can take place in open or closed bioreactors (e. g. fluidized bed reactor, packed bed reactor, and rotating biological contactor) in which diverse microorganisms (e. g. *Pseudomonas*, *Acinetobacter*, *Bacillus*, and *Alcaligene*) through different pathways (e. g. hydrolytic, oxidative, reductive, or substitution/transfer)[15, 22] use CN^- as a nitrogen source [2, 3, 12, 17], with the presence of an additional carbon source (e. g. glucose, fructose, sodium acetate, or whey) for their growth[10, 12, 14, 18-21]. Nonetheless, our research group has demonstrated the feasibility of a microbial consortium (containing *Bacillus* sp.) able to form a biofilm, which tolerates and biodegrades high concentrations of free cyanide ($[CN^-] = 0.3 g/L$) as a sole carbon and nitrogen source[23].

On the other hand, rotating biological contactors (RBC) are commonly used for industrial wastewater treatment due to their efficiency, low operational cost, and low maintenance cost[4, 14, 20, 21, 24]. Their performance for CN^- biological removal has been studied obtaining promising results. Sirianuntapiboon and Chuamkaew[15] reported a 90% biological removal when $[CN]_i = 0.04 g/L$, Jumbo and Nieto[19] obtained a 85.63% biological removal when $[CN^-]_i = 0.280 g/L$, and Guamán and Nieto[24] reported a 96.89% biological removal when $[CN^-]_i = 0.300 g/L$.

RBC is an open bioreactor with a series of disks supported in a horizontal axis. The disks are partially submerged in the wastewater and allow the formation of a biofilm on its surface. So, the biofilm is capable of resisting, assimilating, and degrading hazardous compounds such as CN^- [14, 18, 25, 26]. Nevertheless, during the initial stages of CN^- biological removal, biofilm

development could be limited by high concentrations of CN^- present on gold mine wastewater[27, 28].

Mathematical modeling is a powerful tool that allows the understanding and prediction of biomass development and degradation capacity of organic compounds or hazardous substances. Consequently, bioreactor operation can be optimized, unknown mechanisms can be studied, and new bioreactors can be designed[29-33].

Most of the mathematical models used to understand and predict wastewater treatment in RBC have been developed during the continuous operation of the bioreactor, with a fully formed biofilm and considering a steady state condition[31-37]. These models usually consider substrates' diffusion into the biofilm and the substrate consumption model usually considers that biodegradation is limited by the substrate concentration, which can be explained by Monod's equation[29, 31]. However, a model able to describe biofilm growth during its initial stages in an RBC under non-steady state conditions has not been reported to our knowledge.

On the other hand, the development of mathematical models requires both kinetic and transport parameters, which present specific units and a range of values[29]. The value of each parameter depends on several features like the type of microorganism and the bioprocess working conditions such as contaminant concentration, carbon concentration, disc rotational speed, medium viscosity, biofilm thickness, among others[30, 31]. Until now, kinetic and transport parameters have not been reported during CN^- biodegradation in an RBC.

Thus, in order to better understand the CN^- biological removal process the present work focused on experimentally determined kinetic and transport parameters such: maximum specific growth rate (μ_{max}), saturation constant (K_{CN^-}), observed biomass yield (Y'_{X/CN^-}), maximum specific rate of consumption (q_{max}), biofilm-loss coefficient (b'), CN^- diffusion coefficient within the biofilm

(D_f), mass transfer coefficient (k), and CN^- flux (J_{CN^-}) for the development of a non-steady state mathematical model and simulation of CN^- biodegradation and biofilm growth during a batch culture using a RBC.

2. Materials and methods

2.1 Experimental procedures

Batch cultures were developed in a RBC (Fig. 1), which has five independent compartments. Four of these compartments (C_1, C_2, C_3 and CL) were equipped with two wood disks each, which were submerged 40.5%, and located on a horizontal axis. In order to separate C_1, C_2, C_3 from CL, compartment C_4 was left empty. Then, a solution composed of: 83% gold mine wastewater (0.3gCN^-/L, final concentration) (Table A.1), 2% liquid culture media (Table B.1), and 15% inoculum (2.2 x 10^7 M.O./mL and 0.3gCN^-/L)[23] was added to compartments C_1, C_2, and C_3. Thus, free cyanide final concentration in the compartments C_1, C_2, and C_3 was 0.295g CN^-/L. Compartment CL was fed with a solution composed of 98% gold mine wastewater (0.3gCN^-/L, final concentration) and 2% liquid culture media without inoculum.

Eight batch cultures were carried out in total, giving 24 assays and 8 control tests. The working conditions for the batch cultures are described in Table 1.

Each batch culture lasted until CN^- concentration was stabilized (three days). After that, in order to maintain $[CN^-]_i$=0.3g/L and 40.5% disc submersion, 0.534L was drained from each compartment, and the same volume was replaced using a Cole-Parmer peristaltic pump. The solution contained 93.63% mining effluent (0.98gCN^-/L) and 6.37% liquid culture medium. Moreover, after batch cultures 4 and 6, the total working volume (1.7L) was replaced because the liquid at the end of the 3th and 5th batch cultures were turbid, which made difficult to quantify free cyanide and biomass in the liquid.

2.2 Analytical determinations

A coverslip was used to measure biofilm thickness (L_f) on three representative points for each disc every day (Fig. 2). After that, the coverslips were dried at room temperature and then stained with violet dye. Then, biofilm thickness was observed in an Olympus-TV0.63XC microscope with 4X magnification, which was coupled with an Olympus-4B03835 camera. Finally, biofilm thickness measurements were established (cm) by iWorks 2.0 (Fig C.1-C.8).

Moreover, every two hours 1mL of liquid was taken from each compartment in order to quantify biomass concentration at 540nm using UV-VIS (Thermo Scientific Helios Epsilon.). Then at the beginning and at the end of each batch culture biofilm density (wet basis) and biomass on the discs (X_D, dry basis) were determined. To do that, biofilm was scraped from the discs with a spatula and collected in an Eppendorf tube until reach 0.015mL. Before samples were dried at 105°C for 24h in a Memmert stove UN 450 [39], them were weighted first to obtain biofilm mass so biofilm density [40] could be established.

Free cyanide concentration was quantified every two hours for each compartment by two methods. First, [CN^-]>0.05g/L was measured by titration using silver nitrate ($AgNO)_3$ as titrant and potassium iodide (KI, 5%) as indicator [41]. Second, [CN^-]<0.05g/L was measured by an ion-selective cyanide electrode (Thermo Scientific Orion 9606BNWP) [42]. pH was established for each compartment every 0.5h with Hanna Instruments (HI 8424) pH meter. Medium density (ρ) and dynamic viscosity (μ_d) were measured with a densimeter (Chage # 1981) and a viscometer (Brookfield DV-I) at the end of the eighth batch culture, respectively.

2.3 Mathematical procedures

2.3.1 Biofilm kinetic parameters

Microbial specific growth rate (μ) was obtained from the experimental data of biomass concentration (X) from the liquid medium with Eq.1. Then, CN^- concentration and microbial growth rate were linearized ($1/CN^-$ and $1/\mu$) according to Monod's equation (Eq.2)[41]. Finally, saturation constant (K_{CN-}) and maximum microbial growth rate (μ_{max}) were obtained.

$$\mu = \frac{\mathrm{Ln(X)} - \mathrm{Ln}(X_0)}{(t - t_0)} \quad \text{(Eq.1)}$$

$$\frac{1}{\mu} = \frac{K_{CN-}}{\mu_{max}} \frac{1}{[S]} + \frac{1}{\mu_{max}} \quad \text{(Eq.2)}$$

Observed biomass yield ($Y'_{X/CN-}$) was determined from the experimental data of both biomass concentration on the discs (X_D) and CN^- (Eq.3)[31].

$$Y'_{X/CN^-} = -\frac{\Delta X_D}{\Delta CN^-} \quad \text{(Eq.3)}$$

Free cyanide maximum specific rate (q_{max}) was established from Eq.4, which relates both maximum microbial growth rate (μ_{max}) and observed biomass yield (Y'_{X/CN^-})[31].

$$q_{max} = \mu_{max} / Y'_{X/CN^-} \quad \text{(Eq.4)}$$

Biofilm specific loss rate (b') was obtained from Eq.5, which considers two mechanisms: microbial decay rate in the liquid (μ_{dec}) and biofilm's detachment due to shear stress (b_{des})[31].

$$b' = \mu_{dec} + b_{des} \quad \text{(Eq.5)}$$

The microbial decay rate (μ_{dec}) was determined by Eq.6 during the death phase when the microbial population declined and CN^- consumption was not significant in the liquid medium.

$$\mu_{dec} = \left(\frac{\mathrm{Ln(X)} - \mathrm{Ln}(X_0)}{(t - t_0)}\right)_{dec} \quad \text{(Eq.6)}$$

The specific biofilm-detachment loss coefficient (b_{des}) used was Eq.7 for biofilm thickness > 0.003cm [31].

$$b_{des} = 8.42 * 10^{-2} \left(\frac{\sigma}{1 + 433.2(L_f - 0.003)}\right)^{0.58} \quad \text{(Eq.7)}$$

2.3.2 Free cyanide biological removal parameters

Free cyanide diffusion coefficient in water (D_w) was determined following an empirical correlation by Wilke and Chang (Eq.8)[44].

$$D_w = \frac{(117.3*10^{-8})(\varphi M_B)^{0.5} T}{\mu_d v_A} \quad \text{(Eq.8)}$$

The shear stress was determined from Eq.9[30].

$$\sigma = \frac{\mu_d * v_A}{Z} \quad \text{(Eq.9)}$$

Free cyanide diffusion coefficient within the biofilm (D_f) was obtained with Eq.10, where the correction factor (*f*) used was 0.8 [29, 31].

$$D_f = f D_w \quad \text{(Eq.10)}$$

Mass transfer coefficient (k) on biofilm's surface was given by Eq.11[44].

$$k = \frac{1}{L}\int_0^L k(x)dx \quad \text{(Eq.11)}$$

Resolving Eq.11, mass transfer coefficient (k) was obtained by Eq.12.

$$k = 0.664\, Sc^{-\frac{2}{3}}\, Re_d^{\frac{1}{2}} \sqrt{\frac{v^2}{R_d L}} \quad \text{(Eq.12)}$$

Kinematic viscosity (v) was determined by Eq.13.

$$v = \frac{\mu_d}{\rho} \quad \text{(Eq.13)}$$

Local Reynolds number (Re_d) was given by Eq.14.

$$Re_d = \frac{(\omega r) R_d}{v} \quad \text{(Eq.14)}$$

Schmidt number was obtained by Eq.15.

$$Sc = \frac{v}{D_w} \quad \text{(Eq.15)}$$

Free cyanide flux (J_{CN^-}) within the biofilm was determined from the pseudo-analytical solution proposed by Rittmann and McCarty[45] (Eq.16). This equation describes substrate's flow inside

a biofilm of any thickness, where η is the effective factor. Equation 16 considered that the concentration of the substrate reaches the steady state within the biofilm[31, 44].

$$J = \eta q_{max} X L_f \frac{[CN^-]_S}{K_{CN^-} + [CN^-]_S} \quad \text{(Eq.16)}$$

2.3.2 Biofilm growth mathematical model

The mathematical model that describes biofilm growth was developed from a mass balance (Eq.17) [31] considering:

- Biofilm growth takes place in a non-stationary state.
- CN^- biodegradation does not take place on the liquid.
- Biofilm density remains constant over time.
- Biofilm detachment was caused by microbial decay and shearing stress.

$$[Rate\ of\ accumulation] = [Rate\ in] - [Rate\ out] + [Rate\ of\ production] - [Rate\ of\ consumption] \quad \text{(Eq.17)}$$

Since a batch culture was carried out, both the mass entering and leaving the system were zero, and Eq.18 applies.

$$\frac{d(Xdz)}{dt} = \mu\,(Xdz) - b'(Xdz) \quad \text{(Eq.18)}$$

Microbial specific growth rate (μ) was replaced by the Monod's equation[43] in order to obtain Eq.19.

$$\frac{d(Xdz)}{dt} = \mu_{max}\left(\frac{[CN^-]}{K_{CN^-} + [CN^-]}\right)(Xdz) - b'(X_f\,dz) \quad \text{(Eq.19)}$$

Maximum microbial specific growth rate (μ_{max}) was replaced in Eq.19 to obtain Eq.20.

$$\frac{d(Xdz)}{dt} = q_{max}\,Y'_{x/CN^-}\left(\frac{[CN^-]}{K_{CN^-} + [CN^-]}\right)(X\,dz) - b'(X\,dz) \quad \text{(Eq.20)}$$

Then, $-r_{ut} = q_{\max X}\left(\frac{[CN^-]}{K_{CN^-} + [CN^-]}\right)$ was replaced into Eq.20 and was integrated between the limits of z=0 to z=L_f.

$$\int_0^{L_f} \frac{d(X\,dz)}{dt} = Y'_{x/\mathrm{CN}^-} \int_0^{L_f} -r_{ut}\,dz - \int_0^{L_f} \mathrm{b}'(X\,dz) \quad \text{(Eq.21)}$$

Finally, after solving Eq.21, the model that described the growth and decay of a biofilm in a RBC was obtained (Eq.22).

$$\frac{d(XL_f)}{dt} = (Y'_{x/\mathrm{CN}^-}J) - \mathrm{b}'(X\,L_f) \quad \text{(Eq.22)}$$

2.3.3 Mathematical model for free cyanide biological removal

Equation 23 was used to describe free cyanide transportation and consumption. The mass balance of free cyanide in a non-stationary state was considered, assuming that [31, 44]:

- RBC working volume remains constant.
- CN^- is distributed uniformly in the liquid medium, and its diffusion is carried out from the liquid to the biofilm.
- CN^- biodegradation is carried out only by the biofilm.

$$hV\frac{d[\mathrm{CN}^-]}{dt} = JaV \quad \text{(Eq.23)}$$

Free cyanide flux inside the biofilm (Eq.16) was replaced in the Eq.23 and Eq.24 was obtained.

$$hV\frac{d[\mathrm{CN}^-]}{dt} = \eta q_{max} X\,L_f \frac{[\mathrm{CN}^-]_S}{K_{\mathrm{CN}^-} + [\mathrm{CN}^-]_S} aV \quad \text{(Eq.24)}$$

2.3.4 Simulation

Free cyanide flux within the biofilm in the third dimension was simulated using Eq.16 which depends on both biofilm thickness and $[CN_i^-]$.

Biofilm growth was simulated using Eq.22 under high (0.450gCN^-/L) and low (0.150gCN^-/L) concentrations. Finally, CN^- biodegradation was simulated with Eq.24 under the fixed conditions of 0.1mm of biofilm thickness and 0.450gCN^-/L.

2.3.5 Models validation

Determination coefficient (r^2)[46], average relative error (ARE)[46], and Marquardt's percent standard deviation (MPSD)[47] were used to establish fit and error between mathematical models and its experimental data.

2.4 Data analysis

Microsoft Excel 16.0 was used for data processing and Wolfram Mathematica[48] was used for modeling and simulation.

3. Results and discussion

3.2 Biofilm growth

Figure 3 shows biofilm thickness growth during CN^- biodegradation without an additional carbon source. The biofilm grew exponentially until day 16 (batch 4) and its maximum thickness was 0.0292cm (from day 1 to day 16). After that, stationary phase (from day 17 to day 36), the biofilm underwent growth and destruction ($L_f = 0.0231 - 0.0290$ cm).

Luque[2] suggested the addition of an alternative carbon source during CN^- biodegradation because of its high toxicity. Furthermore, Singh and Balomajumder[11] stated that microorganisms are able to biodegrade cyanide as a nitrogen source to a maximum concentration of 0.150g/L. Additionally, Mekuto[12] reported that microorganisms are able to tolerate 0.4gCN^-/L as nitrogen source, but affected its biodegradation. However, the microbial consortium used in this study was able to use 0.3gCN^-/L as sole carbon and nitrogen sources allowing its growth and maintenance.

On the other hand, when CN^- was insufficient in the liquid medium, the biofilm thickness started to reduce and the smallest value registered was L_f=0.0217cm (batch 3), which explains the necessity of CN^- for the biofilm to grow (Fig. 3). Moreover, according to Sirianuntapiboon et

al.[14] when biofilm's growth is above 0.3cm, higher detachments or losses between 0.1 to 0.2cm can be registered, whereas in our study this was not detected.

3.3 Free cyanide biological removal (%B.R.)

The highest percentage of CN^- biological removal occurred during the first two days for all the experiments, reaching an average biological removal of 94.0%. Subsequently, the B.R. decreased slowly until the third day when it finally stabilized, giving a total B.R. of 96.36% (Fig. 4). This high B.R. was favored by the low density of the biofilm (ρ=0.11g/cm^3)[30, 49]. However, complete CN^- biodegradation was not possible due to low mass transfer from the liquid to the biofilm during the third day and small biofilm thickness.

Singh and Balomajumder[11], Khamar et al.[50], and Razanamahandry et al.[10] established that high initial concentrations of cyanide (>0.150gCN^-/L) increase its toxicity; as a consequence, CN^- biological removal decreases. However, this research proved that an initial concentration of 0.3 gCN^-/L and without an additional carbon source did not affected CN^- biodegradation by the biofilm, and also allowed its growth, development, and maintenance. Moreover, CN^- B.R. was higher than that registered by Sirianuntapiboon and Chuamkaew[14] (B.R.=93.6%, organic matter as carbon source), and Jumbo and Nieto[18] (B.R.=85.63%, sodium acetate as carbon source), during a continuous culture in a rotating biological contactor. On the other hand, Guamán and Nieto[23] demonstrated the potential of the same microbial consortium to biodegrade CN^- without an additional carbon source. They reached 83.89% of CN^- removal using a continuous culture and a fully formed biofilm[23]. In contrast, this work confirmed that for biofilm growth with a batch culture and using the same bioreactor, microbial consortium, and without an additional carbon source, CN^- B.R. increased by more than 10.0% (B.R.=96.36%), even with a small biofilm thickness (0.0292cm.).

3.4 Transport and kinetic parameters

3.4.1 Maximum specific growth rate (μ_{max})

The maximum specific growth rate obtained for the microbial consortium (containing *Bacillus* sp.) was 0.01h^{-1}. The same value was obtained by Orellana[51] during the biodegradation of 0.3gCN^-/L in Erlenmeyer flasks containing the same culture media and microbial consortium as well. These confirm the ability of the microbial consortium to develop and tolerate high concentrations of CN^- without requiring an additional carbon source.

On the other hand, the value obtained in this investigation was lower than the maximum specific growth rate reported by Mekuto et al.[12] (*B. vulgaris*, $\mu_{max} = 0.12h^{-1}$) and Luque-Almagro[52] (*P. pseudoalcaligenes CECT53*, μ_{max}= 0.03 h^{-1}) after using free cyanide ($[CN^-]_i = 0.4\ g/L$ and $0.05\ g/L$, respectively) as nitrogen source. These higher values of μ_{max} could be related to the additional carbon source being agro waste [12] and acetate [52], rather than only having CN^- for a carbon source. However, our research reports for the first time the capacity of a microbial consortium (containing *Bacillus* sp.) to tolerate and biodegrade high concentrations of CN^-, present in gold mine wastewater, as sole carbon and nitrogen source.

3.4.2 Free cyanide saturation constant (K_{CN-})

The saturation constant was $K_{CN-} = 0.035 g/L$ showing that CN^- initial concentration affected the affinity of the biofilm for this compound. This value was higher than that obtained by Singh and Balomajumder[11] ($K_{CN-} = 0.002 g/L$) when using 0.15gCN^-/L as nitrogen source and phenol as carbon source. Furthermore, Razanamahandry et al.[53] reported K_{CN-}=0.364g/L after using $[CN_i^-] = 0.06$g/L as a nitrogen source, glucose as an additional carbon source, and a microbial consortium. So high CN^- concentrations increased K_{CN-} value thereby reducing the affinity of microorganism for CN^-, and showing its toxic effect as well. Nonetheless, as described in 3.3 a high CN^- B.R. was achieved for this work.

3.4.3 Observed biomass yield from free cyanide (Y'_{X/CN^-})

The average observable yield for the eight batch cultures indicated that 2.81 grams of biomass were produced per gram of CN^- consumed, which is higher than the biomass-carbon yield reported by Vasiliadou et al.[33] ($Y_{X/TOC} = 1.4\ g_{biomass}/g_{TOC}$) during the treatment of agro-industrial effluents using a RBC. Likewise, Vasiliadou et al.[33] proposed a biomass-nitrogen yield between 0.92 and 2.7 $g_{biomass}/g_N$, which is slightly lower compared to the observable yield obtained in this study.

In addition, the yield obtained shows that CN^- was used properly since the biomass adhered to the discs was stable, and it did not show considerable detachments (Fig. 3).

3.4.4 Free cyanide maximum specific rate consumption (q_{max})

Free cyanide maximum specific rate consumption was $0.083\ gCN^-/g_{biomass} - d$ meaning that microorganisms slowly biodegrade CN^- compared to other compounds, such as glucose by *Pseudomonas putida* (q_{max}=0.95gsubstrate/gbiomass-d)[54]. This behavior is attributed to a higher maximum microbial growth rate ($\mu_{max} = 1.21h^{-1}$) and a lower observed biomass-substrate yield ($Y'_{X/S} = 0.731 g_{biomass}/g_{sustrate}$), thus fulfilling the Pasteur effect[31, 53, 55].

3.4.5 Biofilm global detachment coefficient (b')

The biofilm overall coefficient loss was b'=$0.006h^{-1}$ and was mostly affected by microbial decay (μ_{dec}=$0.004h^{-1}$) rather than biofilm detachment (b_{det}=$0.002h^{-1}$). Compared with the value reported by Wanner et al.[29] (b'=$0.33h^{-1}$) for a full mix bioreactor, it is evident that biofilm loss observed in Fig. 3 was affected mostly by the low concentration of nutrients rather than the detachment caused by the shearing stress produced by discs' rotational speed.

For this study b_{det} was lower than McCarty and Rittmann[31] (b_{det}=$0.0035h^{-1}$) for moderate shearing stress. It confirms that the rotational speed (5rpm) proposed by Guamán and Nieto[23]

and used in this study, allowed the maintenance of a homogenous biofilm thickness by the reduction of tangential tension that occurs from the liquid medium to the biofilm. Whereas, μ_{dec} was in the range between 0.002 to $0.067\mathrm{h}^{-1}$ proposed by Wanner and Reichert [56] and Vasiliadou[33]. Thus, biofilm loss was caused by nutrients decrement rather than CN^- toxicity[11]. In addition, it is evident that the initial CN^- concentration used in this study was not high enough to cause an acceleration in microbial death [57], but it allowed biofilm's growth and maintenance (Fig. 3) [56].

3.4.6 Free cyanide molecular diffusion coefficient in water (D_w) and within the biofilm (D_f)

The free cyanide molecular diffusion coefficient in water and the diffusion coefficient within the biofilm were $D_w = 0.8\mathrm{cm}^2/\mathrm{d}$ and $D_f = 0.64\mathrm{cm}^2/\mathrm{d}$, respectively; which are equal to those reported by Pylnika and Dueck[32] during the treatment of ammonia present in wastewater using an RBC. Both studies used industrial effluent as a solvent (water), and a similar correction factor (f = 0.8) to describe the diffusion of the contaminants within the biofilm.

As a result, it shows clearly that CN^- diffused easily in water, rather than within the biofilm where its diffusion decreases due to the presence of solids (e. g. biomass, EPS, minerals)[31, 32]. Wanner[29] obtained a higher substrate diffusion coefficient within the biofilm ($\mathrm{D_f} = 1.0\mathrm{cm}^2/\mathrm{d}$) due to its density ($\rho = 0.10\mathrm{g/cm}^3$) being lower than ours ($\rho = 0.11\mathrm{g/cm}^3$). However, even though our biofilm density was slightly higher, CN^- could diffuse without difficulty into the biofilm facilitating its biodegradation.

3.4.7 Local mass transfer coefficient (k)

The local mass transfer coefficient on biofilm's surface was 9.750cm/d for a system that worked in batch culture and in laminar conditions (Re= 363.81 < 2100) [29, 56]. This is slightly lower than that reported by Beg et al.[58] k=10.17cm/d for a fixed-bed bioreactor using continuous

culture. Thus, in order to increase mass transfer from the liquid to the biofilm the system should be switched to continuous culture after the fifth batch culture (Fig. 3) which will allow the maintenance of high CN^- concentration gradient and generate a turbulent regime that will favor mass transfer, biofilm growth and maintenance and consequently, a better biological removal of CN^- from gold mine wastewater[29, 59, 60].

3.4.8 Free cyanide flux within the biofilm (J)

Free cyanide flux within the biofilm in a non-stationary state was determined on the basis of CN^- concentration and biofilm thickness experimental data. In addition, it considered that CN^- transport within the biofilm was carried out in both the diffusion layer (L) and within the biofilm (L_f).

As seen in Fig. 5, the maximum CN^- flow within the biofilm was $J = 4.9x10^{-5}$g/cm^2-d when CN^- concentration and biofilm thickness were $0.3gCN^-/L$ and 0.0292cm, respectively. Free cyanide flux decreased ($J = 2x10^{-5}g/cm^2 - d$) as biofilm thickness was reduced ($L_f = 0.015cm$) despite the high concentration of free cyanide ($0.3gCN^-/L$) in the wastewater. This flow behavior was similar to that reported by Kim and Cui[61] during the biodegradation of ammonia and organic compounds in a sequencing batch reactor (SBR). They established that when biofilm thickness is small substrate flux within it decays and vice versa, even when there is a high concentration of substrate in the medium[61]. Likewise, McCarty and Rittmann[31] pointed out that the substrate flux within the biofilm decays due to the small biofilm thickness. However, in our study, it should be noted that when CN^- concentration in the liquid medium reached 0.018gCN^-/L on the second day, CN^- flux began to fall ($J = 1.8x10^{-5}g/cm^2 - d$) despite biofilm thickness being at its maximum ($L_f = 0.0292$cm). This flux behavior explains that CN^- had less accessibility from the liquid to the diffusion layer or biofilm's surface and

within the biofilm as well. As consequence, from day two to three CN^- biological removal was 2.36% (Fig. 4).

3.5 Mathematical modeling and simulation

3.5.1 Biofilm growth modeling

Equation 25 described biofilm growth and development from day 1 to 36 (Fig. 6). The biofilm grew exponentially until day 16 (1st to 4th batch culture, Fig. 6). Moreover, the model adjusted to biofilm growth and death registered from day 17 to 36 (5th to 8th culture). Consequently, the determination coefficient for our biofilm growth model was 0.90. In addition, according to Marquardt's standard deviation percentage (MPSD=10.97), the model represents 89.03% of the experimental data, which is better than that registered by Singh and Balamajumder[11] (MPSD=13.73). Furthermore, the average relative error (ARE=7.89) indicated that the parameters generated a model that constitutes 92.11% of the experimental data. It should be noted, as shown in Fig. 6, that the model does not describe the detachment of the biofilm. Therefore, the error between both the model and the experimental data can be reduced by maintaining the initial concentration of CN^-, which will avoid the release of the biofilm (5-8 batch) due to the decrease of nutrients. Pylnika and Dueck[32] proposed a mathematical model for biofilm growth during wastewater treatment accounting for biomass yield, biofilm density, substrate concentration, Michaelis–Menten constant, and the detachment coefficient of the biofilm caused by erosion.

3.5.2 Biofilm growth simulation

Figure 7 shows the simulations carried out for biofilm growth under higher and lower initial concentrations of CN^- ($0.450 g/L$ and $0.150 g/L$, respectively) compared to the proposed model in this study. At 0.450gCN^-/L, the biofilm reached a maximum thickness $L_f = 0.031 cm$, which

does not show a great difference respect the modeled, this can be attributed to an increase in K_{CN^-}, an increase CN^- toxicity, and low mass transfer[14, 30]. Nevertheless, when 0.150gCN^-/L, biofilm thickness decreased ($L_f = 0.027$cm) due to the low contribution of carbon by CN^- and the low mass transfer[51]. The deviation between the model and the simulation using high and low concentrations of CN^- was ±0.002. Additionally, both initial concentrations of 0.300 and 0.450g/L provide enough carbon and nitrogen source for biofilm growth. Moreover, when high concentrations of CN^- are present in the medium its flux also increases within the biofilm and as consequence its thickness increases too. However, due to the absence of an additional carbon source, when CN^- concentration was reduced to half of the tested concentration in this study, it did not provide enough carbon and nitrogen source for the biofilm, resulting in a decrease in its thickness.

3.5.3 Free cyanide biodegradation modeling

Figure 8 compares the experimental data with the mathematical model obtained for CN^- biodegradation by a biofilm in a RBC. The model favorably coupled to the experimental data obtaining a determination coefficient of $r^2 = 0.99$ (Fig. 8). In addition, according to the Marquardt's standard deviation percentage (MPSD=10.17), the proposed model constitutes 89.83% of the experimental data. Also, the average relative error (ARE=7.38) indicated that the possible causes of error between the model and the experimental data were low.

Singh and Balomajumder[11] established a three-half order kinetic for the biodegradation of free cyanide ($[CN^-]_i = 0.15 g/L$) and biomass growth in 250mL flasks. This model considered fewer parameters such as: constant of zero order, rate of product formation, initial biomass concentration, and three-half-order rate constants, than ours. Moreover, its Marquardt's standard

deviation percentage (MPSD=21.54) was higher than ours, indicating that our model is able to better described CN^- biodegradation.

Furthermore, Vasiliadou et al.[34] established a model for pharmaceutical compounds biodegradation using a RBC. This model was based on the previous work of Wanner and Reichert[56], developed under a continuous culture and considering a steady state. Their determination coefficient was lower ($r^2 = 0.756$) than ours, and considered other parameters such as: sorption and desorption constants, pharmaceutical inhibition coefficient, biomass maintenance rate for carbon [31], and experimentally estimated saturation constants for nitrogen and carbon, death rate coefficient, and growth yield coefficient on carbon.

3.5.4 Simulation of CN^- biodegradation

Simulations for CN^- biodegradation for different biofilm thickness and initial CN^- concentration against the established model are presented in Fig. 9. When the conditions were 0.450gCN^-/L and $L_f = 0.0252\text{cm}$, for day one CN^- biological removal was 50.0%, for day two reached 85.3%, and finally was 92.3%. These results show that when CN^- concentration was increased and biofilm thickness maintained, biological removal decreased and the time required increased. This behavior agrees with the simulation developed for biofilm growth at $0.450\text{gCN}^-/\text{L}$.

Nevertheless, our simulation exceeds the biological removal obtained by Mekuto et al.[12] (B.R.=60%) when using *Bacillus* sp., whey as a carbon source, and 0.4gCN^-/L as nitrogen source. The simulation that achieved the highest free cyanide biological removal in a shorter period of time was one with initial conditions of biofilm thickness and CN^- concentration of 0.1cm and 0.450gCN^-/L, respectively. Free cyanide biological removal was 94.3% for day one, 98.0% for day two, and 99.5% for day three. These results agree with experimental trials reported in literature by Najafpour, Zinatizadeh, and Lee[62], Sirianuntapiboon and Chuamkaew[14], Cortez

et al.[63], and Vasiliadou et al.[33], which suggest that the elimination of any contaminant using a RBC depends on biofilm thickness. So, higher thickness favors the biodegradation of CN^- as a carbon and nitrogen source due to the presence of more biomass.

4. Conclusions

Free cyanide biological removal and biofilm growth were achieved during eight consecutive batch processes in a rotating biological contactor. The maximum biofilm thickness was 0.0292cm after the fourth batch (day 16) and mean free cyanide biological removal was 96.36%. Furthermore, experimental kinetic and transport parameters were obtained, such as: maximum specific growth rate (μ_{dec}=0.01h^{-1}), free cyanide saturation constant ($K_{CN-} = 0.035 g/L$), observed biomass yield ($Y'_{X/CN^-} = 2.81\, {}^{g\ biomass}/_{g\ CN-}$), maximum specific rate of consumption ($q_{max} = 0.083\ \mathrm{gCN^-/g_{biomass} - d}$), biofilm loss coefficient ($b' = 0.006 \mathrm{h^{-1}}$), free cyanide diffusion coefficient within the biofilm ($\mathrm{D_f} = 0.64 \mathrm{cm^2/d}$), mass transfer coefficient ($k = 9.750 \mathrm{cm/d}$), and maximum free cyanide flow within the biofilm ($J = 4.9x10^{-5}$g/cm^2-d). These parameters allowed to develop two mathematical models one for biofilm growth and other for free cyanide biodegradation, which successfully coupled with its experimental data r^2=0.90 and r^2=0.99, respectively. Therefore, both models can be used to predict, control, and optimize the development of biofilm growth during free cyanide biological removal present in gold mine wastewater without an additional carbon source, in a rotating biological contactor.

Conflicts of interest

None.

Acknowledgments

The authors thank Universidad Técnica Particular de Loja for the financial support through its annual Research Projects calls 2013, 2014, and 2015 (PROY_QUI_862, PROY_QUI_0016, and PROY_CCNN_1182), and ORENAS S.A. for wastewater sampling. Also, we appreciate the language check and suggestions on the manuscript due by José Flores Uribe, Ph D.

Supplementary material

Appendices A, B, and C.

References

[1] R.R. Dash, A. Gaur, and C. Balomajumder, Cyanide in industrial wastewaters and its removal: A review on biotreatment. Journal of Hazardous Materials. 163 (2009) 1-11.

[2] V.M. Luque-Almagro, C. Moreno-Vivián, and M.D. Roldán, Biodegradation of cyanide wastes from mining and jewellery industries. Current Opinion in Biotechnology, 38 (2016) 9-13.

[3] L.C. Razanamahandry, H. Karoui, H. A. Andrianisa, H. Yacouba, Bioremediation of soil and water polluted by cyanide: A review. African Journal of Environmental Science and Technology, 11 (2017) 272-291.

[4] M. Botz, T. Mudder, and A. Akcil, Cyanide treatment: physical, chemical and biological processes. Advances in Gold Ore Processing, (2015) 1-28.

[5] I. Manso, M.I. Ibáñez, F. de la Peña, L.P. Sáez, V.M. Luque-Almagro, F. Castillo, M.D. Roldán, M.A. Prieto, C. Moreno, Pseudomonas pseudoalcaligenes CECT5344, a cyanide-degrading bacterium with by-product (polyhydroxyalkanoates) formation capacity. Microbial cell factories, 14 (2015) 77.

[6] M.I. Ibáñez, P. Cabello, V.M. Luque-Almagro, L.P. Sáez, A. Olaya, V. Sánchez de Medina, M.D. Luque de Castro, C. Moreno-Vivián., and M.D. Roldán. Quantitative proteomic analysis of Pseudomonas pseudoalcaligenes CECT5344 in response to industrial cyanide-containing wastewaters using Liquid Chromatography-Mass Spectrometry/Mass Spectrometry (LC-MS/MS). 12(3) (2017) 0172908.

[7] V.M. Luque-Almagro, F. Merchán, R. Blasco, M.I. Igeño, M. Martínez-Luque, C. Moreno-Vivián, F. Castillo, M.D. Roldán, Cyanide degradation by Pseudomonas pseudoalcaligenes CECT5344 involves a malate: quinone oxidoreductase and an associated cyanide-insensitive electron transfer chain. Microbiology, 157(3) (2011) 739-746.

[8] V.M. Luque-Almagro, F. Acera, M.I. Igeño, D. Wibberg, M.D. Roldán, L.P. Sáez, M. Hennig, A. Quesada, M.J. Huertas, J. Blom, F. Merchán, M.P. Escribano, S. Jaenicke, J. Estepa, M.I. Guijo, M. Martínez-Luque, D. Macías, R. Szczepanowski, G. Becerra, S. Ramirez, M.I. Carmona, O. Gutiérrez, I. Manso, A. Pühler, F. Castillo, C. Moreno-Vivián, A. Schlüter, R. Blasco, Draft whole genome sequence of the cyanide-degrading bacterium Pseudomonas pseudoalcaligenes CECT5344. Environmental microbiology, 15(1) (2013) 253-270.

[9] A. Akcil, and T. Mudder, Microbial destruction of cyanide wastes in gold mining: process review. Biotechnology Letters, 25(6) (2003) 445-450.

[10] L.C. Razanamahandry, H.A. Andrianisa, H. Karoui, K.M. Kouakou, H. Yacouba. Biodegradation of free cyanide by bacterial species isolated from cyanide-contaminated artisanal gold mining catchment area in Burkina Faso. Chemosphere, 157 (2016) 71-78.

[11] N. Singh, and C. Balomajumder, Batch growth kinetic studies for elimination of phenol and cyanide using mixed microbial culture. Journal of Water Process Engineering, 11 (2016) 130-137.

[12] L. Mekuto, V.A. Jackson, and S.K. Ntwampe, Biodegradation of free cyanide using Bacillus sp. consortium dominated by Bacillus safensis, Lichenformis and Tequilensis strains: A bioprocess supported solely with whey. 2013.

[13] N. Gupta, C. Balomajumder, and V. Agarwal, Enzymatic mechanism and biochemistry for cyanide degradation: a review. Journal of Hazardous Materials, 176(1) (2010) 1-13.

[14] S. Sirianuntapiboon, and C. Chuamkaew, Packed cage rotating biological contactor system for treatment of cyanide wastewater. Bioresource technology, 98(2) (2007) 266-272.

[15] F. Gurbuz, H. Ciftci, and A. Akcil, Biodegradation of cyanide containing effluents by Scenedesmus obliquus. Journal of hazardous materials, 162(1) (2009) 74-79.

[16] B. Tiong, B, Z.M. Bahari, N. I. Lee, J. Jaafar, Z. Ibrahim, and S. Shahir. Cyanide degradation by Pseudomonas pseudoalcaligenes strain W2 isolated from mining effluent. Sains Malaysiana, 44(2) (2015) 233-238.

[17] V. Arutchelvan, R. Elangovan, K. R. Venkatesh and S. Nagarajan. Biodegradation of cyanide using bacillus megaterium. Industrial Pollution Control 21 (2005) 247- 254.

[18] P.X. Jumbo. and D.A. Nieto, Removal of free cyanide present on gold mine wastewater using a rotating biological contactor. Microbes in the Spotlight: Recent Progress in the Understanding of Beneficial and Harmful Microorganisms, (2016) 130.

[19] Hassard, F., J. Biddleab, E. Cartmella, B. Jeffersona, S.Tyrrela, T. Stephenson, Rotating biological contactors for wastewater treatment – A review. Process Safety and Environmental Protection, 94 (2015) 285-306.

[20] M. Huertas, L.P. Sáez, M.D. Roldán, V.M. Luque-Almagro, M. Martínez-Luque, R. Blasco, E. Castillo, C. Moreno-Vivián, I. García-García. Alkaline cyanide degradation by Pseudomonas pseudoalcaligenes CECT5344 in a batch reactor. Influence of pH. Journal of Hazardous Materials, 179(1) (2010) 72-78.

[21] N. Kuyucak, and A. Akcil, Cyanide and removal options from effluents in gold mining and metallurgical processes. Minerals Engineering, 50-51 (Supplement C) (2013) 13-29.

[22] S. Ebbs, S., Biological degradation of cyanide compounds. Current opinion in Biotechnology, 15(3) (2004) 231-236.

[23] M.P. Guamán Guadalima, and D.A. Nieto Monteros, Evaluation of the rotational speed and carbon source on the biological removal of free cyanide present on gold mine wastewater, using a rotating biological contactor. Journal of Water Process Engineering, 23 (2018) 84-90.

[24] K. Al-Ahmady, Effect of organic loading on rotating biological contactor efficiency. International journal of environmental research and public health, 2(3) (2005) 469-477.

[25] E.R.C. Borges, A.B. Rojas, and R.I.M. Novelo, Remoción de materia orgánica en aguas residuales de rastro por el proceso de Contactor Biológico Rotacional. Grasas y aceites (mg/L), 100 (2012) 600.

[26] S. Sirianuntapiboon, Treatment of wastewater containing Cl2 residue by packed cage rotating biological contactor (RBC) system. Bioresource Technology, 97(14) (2006) 1735-1744.

[27] A. Patwardhan, Rotating biological contactors: a review. Industrial & engineering chemistry research, 42(10) (2003) 2035-2051.

[28] P.A. Kadu, and Y. Rao, A review of rotating biological contactors system. IJERA, 2 (2012) 2149-2153.

[29] O. Wanner, H. Eberl, E. Morgenroth, D. Noguera, C. Picioreanu, B. Rittmann, and M. van Loosdrecht, Mathematical modeling of biofilms, IWA publishing, vol 18, 2006.

[30] Z. Lewandowski, and H. Beyenal, Fundamentals of biofilm research. CRC press, 2013.

[31] P. McCarty, and B. Rittmann, Environmental biotechnology: principles and applications, Tata McGraw-Hill Education, 2000.

[32] S.V. Pylnik, and I.G. Dueck, Startup simulation for a rotating biological contactor. Theoretical Foundations of Chemical Engineering, 46(1) (2012) 72-79.

[33] I.A. Vasiliadou, M.I. Pariente, F. Martinez, J.A. Melero, R. Molina, Modeling the integrated heterogeneous catalytic fixed-bed reactor and rotating biological contactor system for the treatment of poorly biodegradable industrial agrochemical wastewater. Journal of Environmental Chemical Engineering, 4(2) (2016) 2313-2321.

[34] I. Vasiliadou, R. Molina, F. Martínez, J.A. Melero. Experimental and modeling study on removal of pharmaceutically active compounds in rotating biological contactors. Journal of Hazardous Materials, 274 (2014) 473-482.

[35] S.V. Pylnik, and I.G. Dueck, Modeling of substrate consumption by a biofilm on the surface of a rotating partially submerged disk. Theoretical Foundations of Chemical Engineering, 45(1) (2011) 13-20.

[36] T. Yamaguchi, M. Ishida, T. Suzuki, Biodegradation of hydrocarbons by Prototheca zopfii in rotating biological contactors. Process biochemistry, 35(3) (1999) 403-409.

[37] J. Famularo, J.A. Mueller, T. Mulligan, Application of mass transfer to rotating biological contactors. Journal (Water Pollution Control Federation), (1978) 653-671.

[38] Dassault Systèmes, Solidworks, Version 26, Waltham, MA, 2018.

[39] C. Arnáiz Franco, L. Isac Oria, and J. Lebrato Martínez, Determinación de la biomasa en procesos biológicos. I Métodos directos e indirectos. Tecnología del agua, 20 (205) (2000) 45-52.

[40] H. Horn, and S. Lackner, Modeling of biofilm systems: a review, in Productive Biofilms. (2014) 53-76.

[41] H. B. Singh, & N. M. M. C. Wasi, Detection and Determination of Cyanide-A Review. International Journal of Environmental Analytical Chemistry, 26:2 (1986), Pp. 115-136.

[42] J. Wang, Analytical Electrochemistry, 3th Ed., New York: John Wiley & Sons, 2006.

[43] J. Monod, The growth of bacterial cultures Annual Reviews, 3 (1949) 371-394.

[44] R.B. Bird, W.E. Stewart, E.N. Lightfoot, Transport Phenomena, Wiley, 2007.

[45] B. E. Rittmann, and P.L. McCarty, Substrate flux into biofilms of any thickness. Journal of the Environmental Engineering Division, 107(4) (1981) 831-849.

[46] D.W. Marquardt, An Algorithm for Least-Squares Estimation of Nonlinear Parameters. Journal of the Society for Industrial and Applied Mathematics, 11(2) (1963) 431-441.

[47] Kumar, K.V., Linear and non-linear regression analysis for the sorption kinetics of methylene blue onto activated carbon. Journal of hazardous materials, 137(3) (2006) 1538-1544.

[48] Wolfram Research, Inc., Mathematica, Version 11.3, Champaign, IL (2018).

[49] S. Sabarunisha Begum, K.V. Radha, Effect of gas–liquid mass transfer coefficient and liquid–solid mass transfer resistance on phenol biodegradation in three phase inverse fluidized bed biofilm reactor. Journal of Environmental Chemical Engineering, 2(4) (2014) 2321-2326.

[50] Z. Khamar, A. Makhdoumi-Kakhki, M.M. Gharaie, Remediation of cyanide from the gold mine tailing pond by a novel bacterial co-culture. International Biodeterioration & Biodegradation, 99 (2015) 123-128.

[51] A.G. Orellana, Biodegradación de cianuro libre en presencia y ausencia de fuente de carbono. Undergraduate thesis, Universidad Técnica Particular de Loja, 2015. Available from: https://bibliotecautpl.utpl.edu.ec/abnetopac/abnetcl.exe/O9575/ID12c504d0/NT1?ACC=116&DOC=3 (unpublished).

[52] V.M. Luque-Almagro, Metabolismo del cianuro y del cianato en Pseudomonas pseudoalcaligenes CECT5344, aplicaciones biotecnológicas. Andalucia. Analistas económicos, (2005) 187-189.

[53] L. C. Razanamahandry, L. Mekuto, V. Bazie, H. A. Andrianisa, H.Karoui, K. Meibom, M. Frutschi, S.K.O. Ntwampe, R.Bernier-Latmani, H. Yacouba. Free Cyanide Degradation Kinetics of Free Cyanide Degradation Kinetics of Cyanide Degrading Bacteria. 2018.

[54] G. Okpokwasili, and C. Nweke, Microbial growth and substrate utilization kinetics. African Journal of Biotechnology, 5(4) (2006) 305-317.

[55] R. Parés, and A. Juárez, Bioquímica de los microorganismos. Reverté, 1997.

[56] O. Wanner, and P. Reichert, Mathematical modeling of mixed-culture biofilms. Biotechnology and bioengineering, 49(2) (1996) 172-184.

[57] D. Taherzadeh, C. Picioreanu, H. Horn, Mass transfer enhancement in moving biofilm structures. Biophysical journal, 102(7) (2012) 1483-1492.

[58] S.A. Beg, M.M. Hassan, M.A.S. Chaudhry, Chromium(VI) inhibition in multi-substrate carbon oxidation and nitrification process in an upflow packed bed biofilm reactor. Biochemical Engineering Journal, 1(2) (1998) 143-152.

[59] R.B. Bird, W.E. Stewart, E.N. Lightfoot, Fenómenos de transporte. Limusa Wiley, 2006.

[60] H. Beyenal, and Z. Lewandowski, Internal and external mass transfer in biofilms grown at various flow velocities. Biotechnology progress, 18(1) (2002) 55-61.

[61] M. Kim, and F. Cui, Use of Nonsteady-state Biofilm Model to characterize heterotrophic and autotrophic biomass within aerobic granules. KSCE Journal of Civil Engineering, 2017: p. 1-6.

[62] G. Najafpour, A. Zinatizadeh, L. Lee, Performance of a three-stage aerobic RBC reactor in food canning wastewater treatment. Biochemical engineering journal, 2006. 30(3): p. 297-302.

[63] S. Cortez, P. Teixeira, R. Oliveira, M. Mota, Rotating biological contactors: a review on main factors affecting performance. Reviews in Environmental Science and Bio/Technology, 7(2) (2008) 155-172.

Figure captions

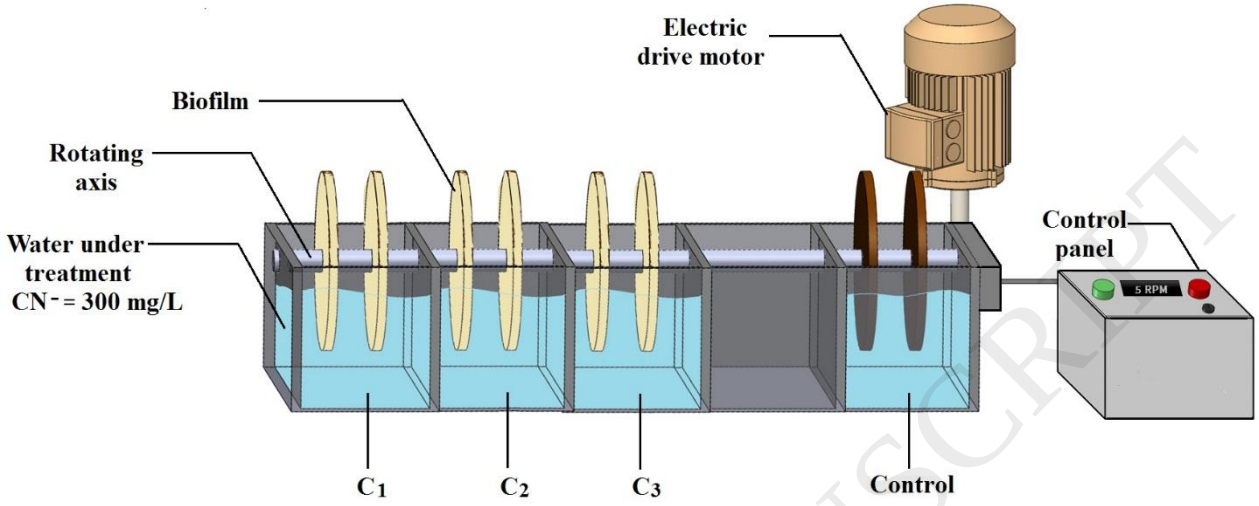

(a)

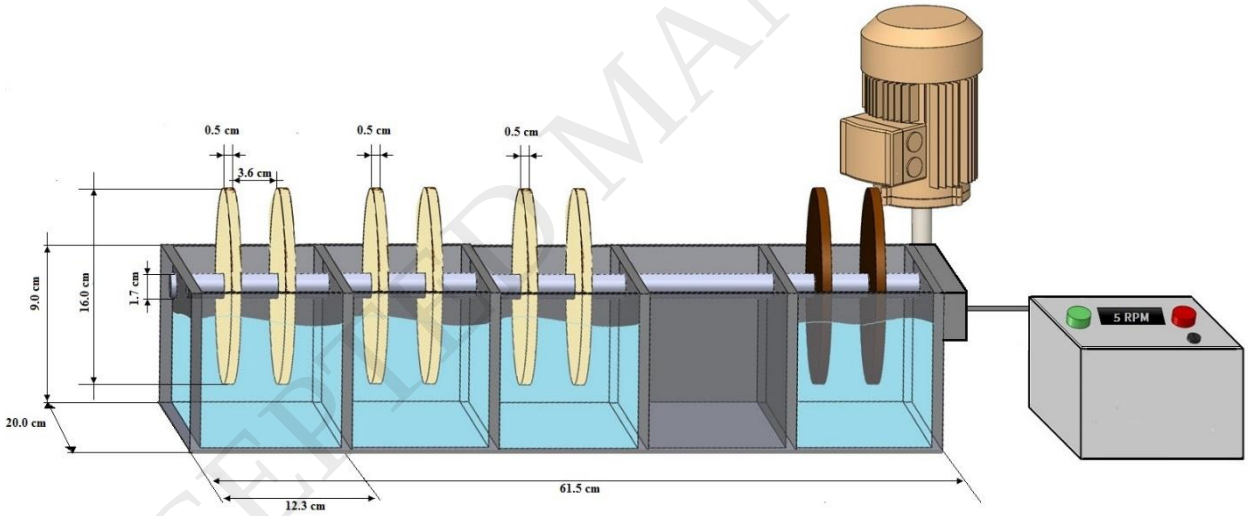

(b)

Fig. 1. (a) Bench-scale rotating biological contactor design and (b) rotating biological contactor measurements.

Source: Solidworks [38].

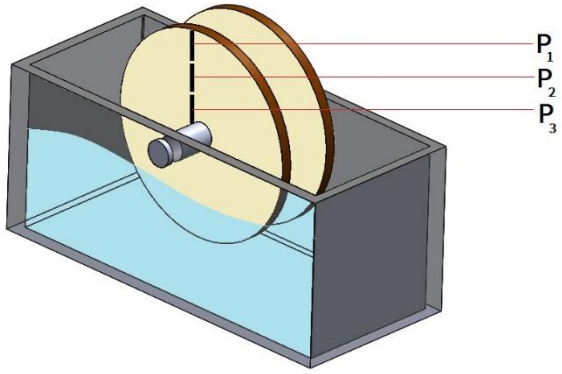

Fig. 2. Sampled points used to determinate biofilm thickness (L_f).

Source: Solidworks [38].

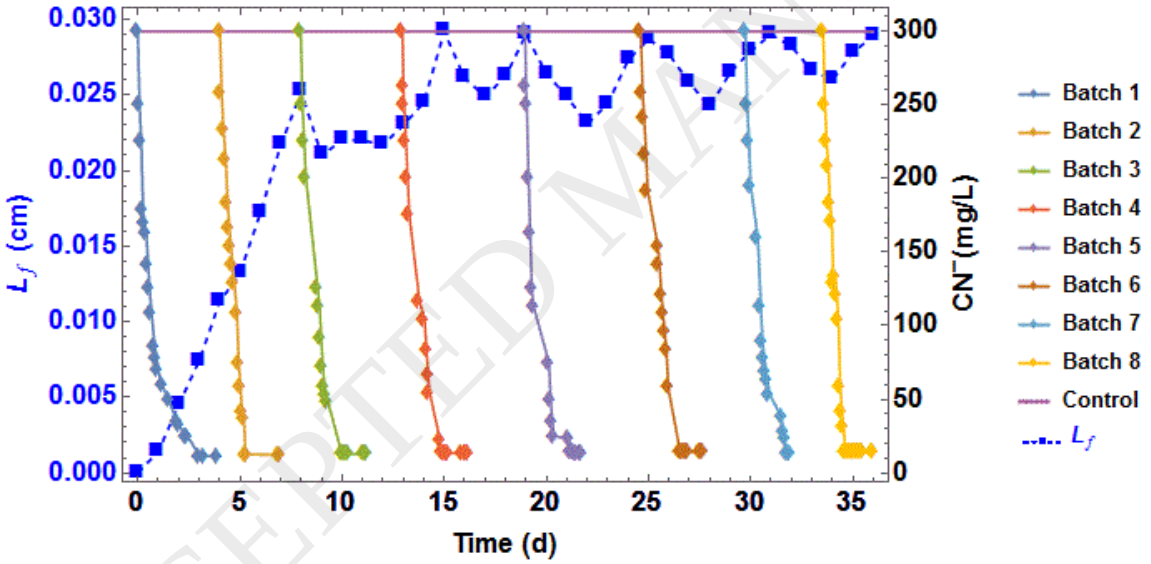

Fig. 3. Comparison between biofilm thickness growth (L_f) (primary axis) with respect to free cyanide biodegradation, and control tests (secondary axis) for eight consecutive batch cultures, using a rotating biological contactor. Mean of 24 assays and 8 controls.

Source: Wolfram Mathematica [48].

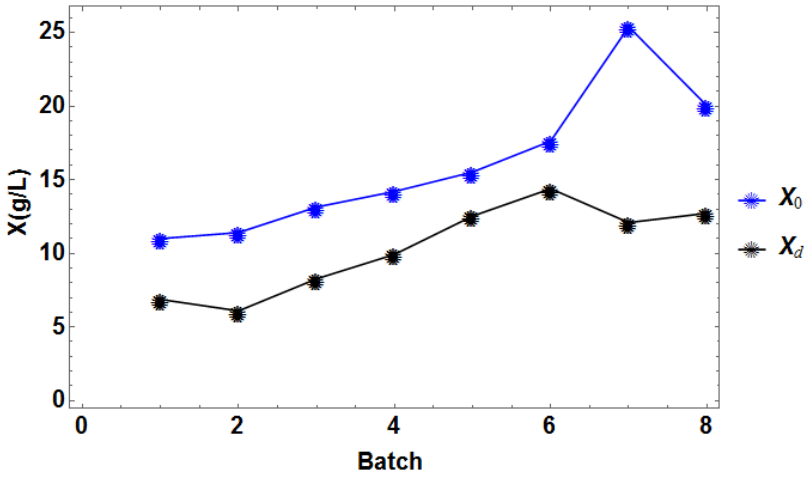

Fig. 4. Biomass concentration in the liquid at the beginning (X_0) and end (X_d) for each batch culture. Mean of 24 experiments.

Source: Wolfram Mathematica [48].

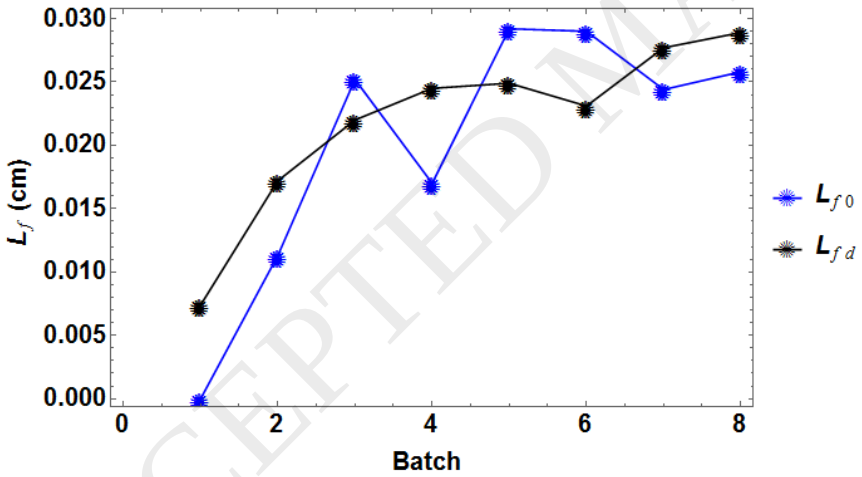

Fig. 5. Biofilm thickness at the beginning (L_{f0}) and end (L_{fd}) of each batch culture. Mean of 24 experiments.

Source: Wolfram Mathematica [48].

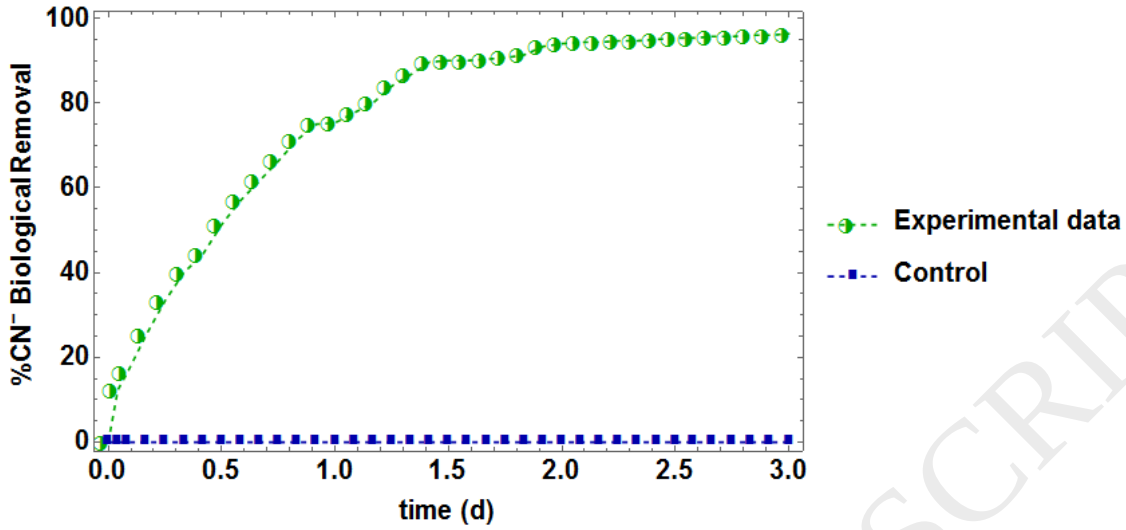

Fig. 6. Mean free cyanide biological removal (%) during a batch culture in a RBC. Mean of 24 experiments and 8 controls.

Source: Wolfram Mathematica [48].

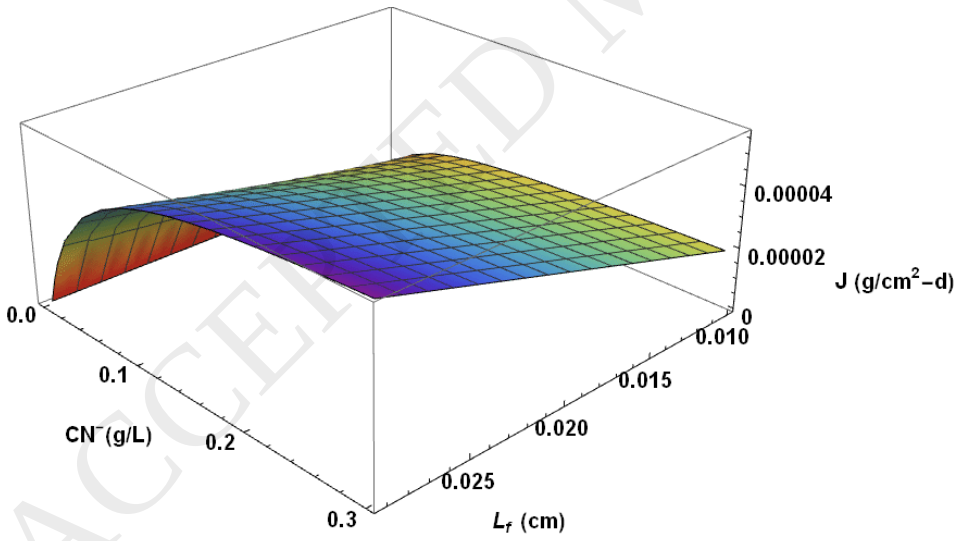

Fig. 7. 3D free cyanide flux (J) simulation within the biofilm using different concentrations of free cyanide (CN^-) and biofilm thickness (L_f).

Source: Wolfram Mathematica [48].

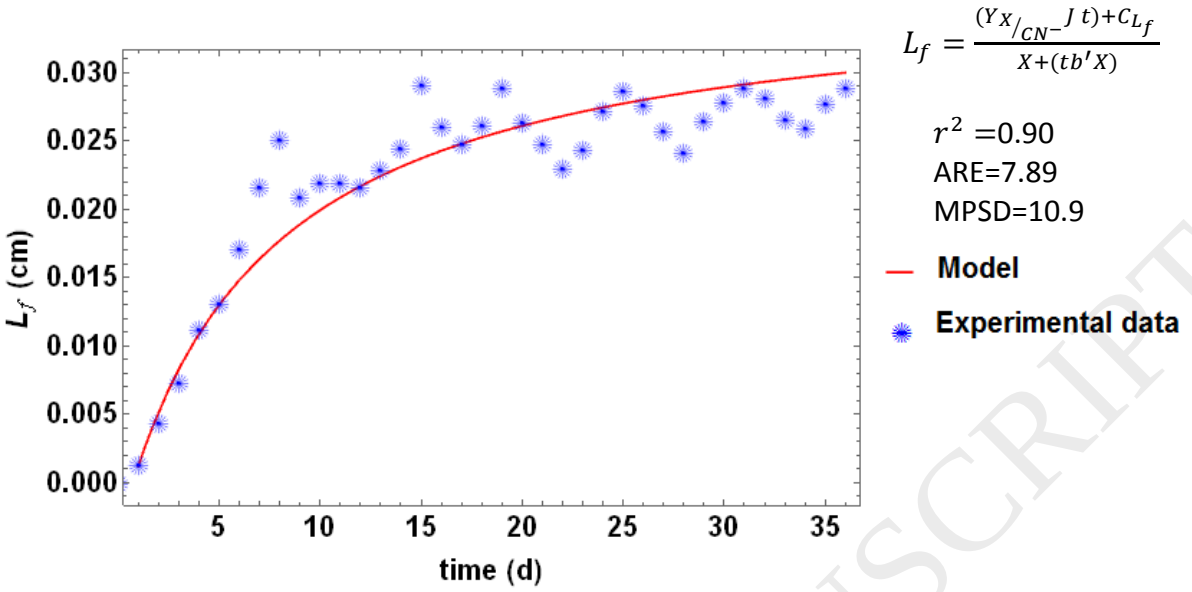

Fig. 8. Comparison between the experimental data and the proposed mathematical model for biofilm growth during CN^- biological removal. Mean of 24 assays and 8 controls.

Source: Wolfram Mathematica [48].

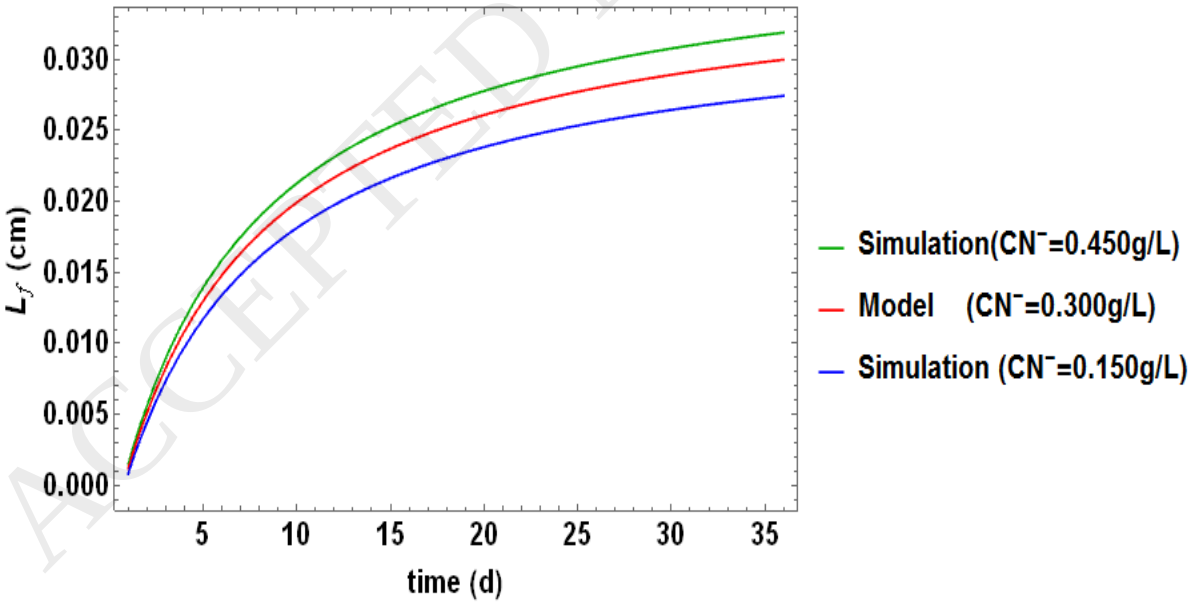

Fig. 9. Comparison between biofilm growth (L_f) model and simulations at different initial concentrations of CN^- (0.450g/L and 0.150g/L).

Source: Wolfram Mathematica [48].

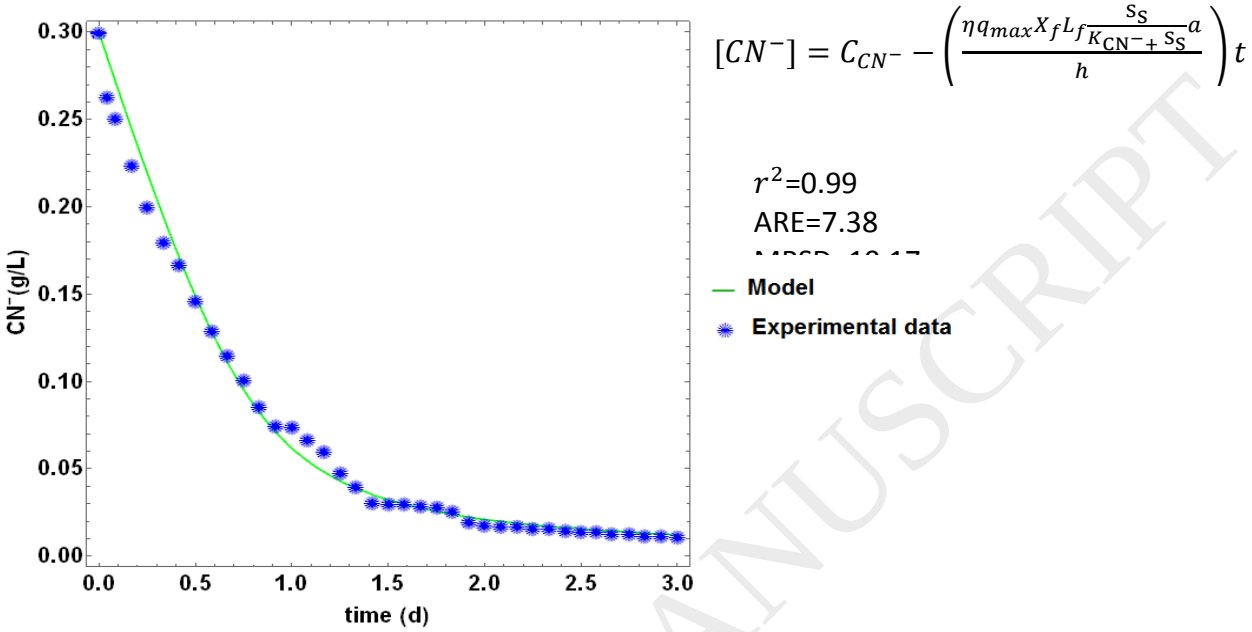

Fig. 10. Free cyanide biodegradation model vs experimental data. Mean of 24 assays and 8 controls.

Source: Wolfram Mathematica [48].

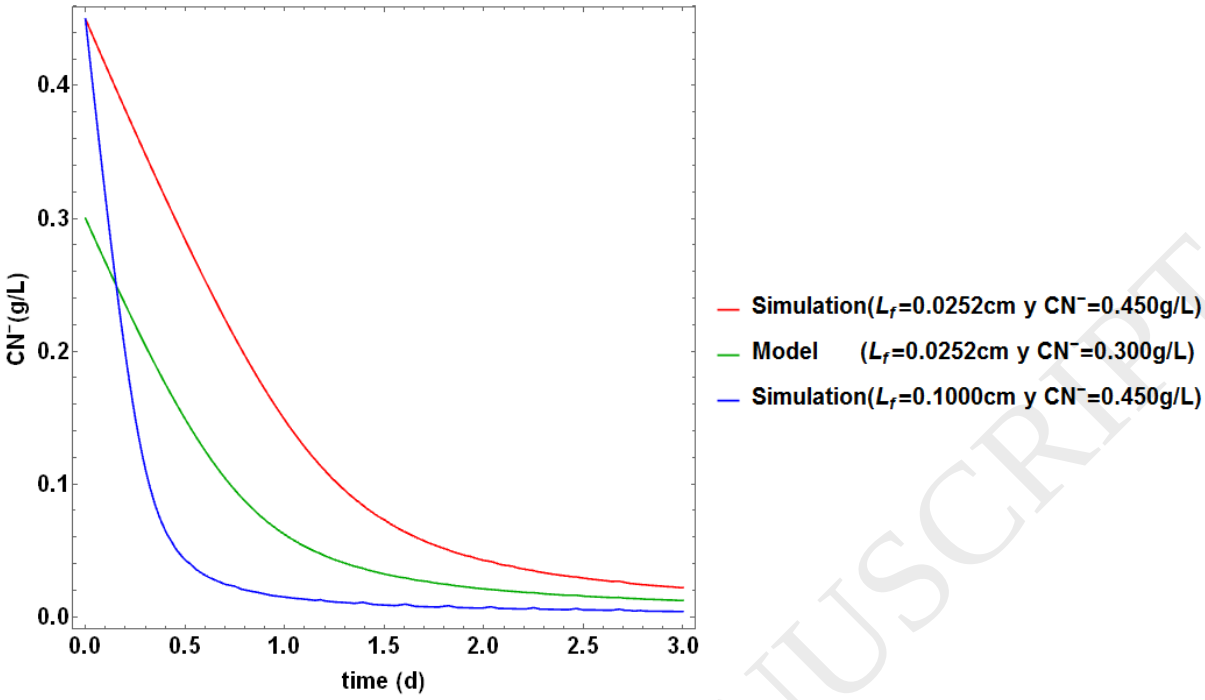

Fig. 11. Simulation of CN^- biodegradation vs the proposed model, for different initial concentrations of free cyanide (CN^-) and biofilm thickness (L_f).

Source: Wolfram Mathematica [48].

Table 1. Batch culture working conditions.

	Parameter	Value	Unit	References
Physical	Temperature	20±5	°C	[23]
	*V_{RBC}	1.7	L	
Chemical	pH	10.5±0.5	-	[23]
	$[CN_i^-]$	0.3	g/L	[23]
Operational	Disk rotational speed (ω)	5	rpm	[23]
	Disk submersion (D. S.)	40.5	%	[35]

*Note: V_{RBC} is the working volume for each compartment for a 40.5% disc submersion.